Bayesian force reconstruction with an uncertain model

Erliang Zhang, Jérôme Antoni, Pierre Feissel

Bayesian force reconstruction with an uncertain model

E. Zhang [a,*], J. Antoni [b], P. Feissel [a]

[a] *Roberval Laboratory of Mechanics, CNRS UMR 6253, University of Technology of Compiègne, France*
[b] *Vibration and Acoustic Laboratory, University of Lyon, F-69621 Villeurbanne, France*

This paper presents a Bayesian approach for force reconstruction which can deal with both measurement noise and model uncertainty. In particular, an uncertain model is considered for inversion in the form of a matrix of frequency response functions whose modal parameters originate from either measurements or a finite element model. The model uncertainty and the regularization parameter are jointly determined with the unknown force through Monte Carlo Markov chain methods. Bayesian credible intervals of the force are built from its posterior probability density function by taking into account the quantified model uncertainty and measurement noise. The proposed approach is illustrated and validated on numerical and experimental examples.

1. Introduction

The knowledge of the force exerted on a mechanical system is an important information in many structural dynamic applications. However, its measurement with transducers is a difficult task in many instances, especially if the measurement is intrusive or if the force is distributed. Instead, vibration responses can be conveniently measured. It is the reason why indirect methods are often preferred, which consist in reconstructing forces based on inverting the model of a mechanical system. In recent years, various model-based force reconstruction methods have been proposed, especially within the context of accurate models (modal model, impulse response function or frequency response function, FRF) [1–8]. Much attention has been paid on the stability of the inversion, for instance by means of the singular value decomposition or the Tikhonov regularization method [3–5]. Antoni [1] illustrates an optimal inverse filter to reconstruct the cylinder pressures of IC engines. Choi [6] compares the performance of the ordinary and generalized cross validation methods and the L-curve criterion in selecting the optimal parameter for Tikhonov regularization. The Kalman filter along with a recursive least-squares algorithm is adopted for the online force reconstruction based on a finite element (FE) model [7]. Gunawan [8] uses a two-step B-splines method to approximate and to regularize an impact-force profile. Besides, attention is also paid to the reconstruction of distributed force based on a modal model in [9,10] using Thikonov regularization and in [11] using mode selection method.

As a matter of fact, the final reconstructed force heavily relies on the quality of the modal model or the FRFs which are inverted and are typically either estimated from experimental modal analysis [12,13] or predicted by a FE model. By virtue of its predictive ability, the FE approach is surely promising in model-based force reconstruction provided a model updating stage [14] is performed before inversion. Nevertheless, even a finely updated model cannot reproduce exactly the real behavior of a structure due to limitations of the model itself. In addition, no matter how precisely a structure's FRFs are measured in the laboratory, these will never correspond perfectly to the actual operating FRFs due to changes in the

* Corresponding author.
E-mail address: erliang.zhang@utc.fr (E. Zhang).

boundary conditions and damping mechanisms when passing from the laboratory environment to practical operating state. As far as the authors know, these aspects have seldom been taken into account in force reconstruction problems despite their importance. A total least-square scheme is used to address the errors associated with the FRF matrix in [5]. Similarly Ref. [15] proposes a discrete modal filter to reduce the error propagation from the biased modal parameters to the reconstructed force.

On account of the presence of measurement noise and modeling error, force reconstruction is tackled within a probabilistic framework. Since measurement noise is inherently aleatory because of nature, and modeling error can be considered as random by epistemic uncertainty due to lack of knowledge, the model error is hereafter called model uncertainty and is considered within a probabilistic context. In the present work, force reconstruction is particularly investigated from a Bayesian perspective by viewing the unknown quantities as random variables or stochastic process [16,17]. This has several advantages. First it endows the unknown force with prior information on the possible range of its values in the form of a probability density function (p.d.f.), which naturally imposes an intrinsic regularization. Second, the Bayesian approach furnishes a rigorous probabilistic framework to account for all possible sources of errors that participate to the uncertainty of the reconstructed force, including the measurement noise and the model uncertainty. As an original contribution, the model uncertainty is considered by following two strategies, firstly encoded at the FRFs level, then at the level of the modal parameters. The first strategy is the simplest, but the second one is found superior when the forward model happens to have a significant level of uncertainty in a certain frequency band. In both cases, Bayesian reconstructions are established for reconstructing the force and jointly quantifying the measurement noise and model uncertainty through Monte Carlo Markov chain (MCMC) methods. Bayesian credible interval on the reconstructed force is systematically delivered, which is of practical use.

The rest of paper is organized as follows. Section 2 introduces some generalities on the force reconstruction algorithm within the Bayesian framework. Section 3 proposes a general Bayesian formulation based on MCMC implementation to reconstruct forces by inverting uncertain FRFs and discusses the role of local regularization. Section 4 proposes a similar approach when reconstruction is carried out under uncertain modal parameters. Finally, Section 5 illustrates the proposed approaches on numerical and experimental examples and conclusions are given in Section 6.

2. Force reconstruction within the Bayesian framework

In this paper, an italic character means a scalar variable, a bold character denotes a vector, and a matrix is expressed by a character enclosed in a bracket. The model-based approach consists in reconstructing the force from measurements based on the physical model of a mechanical system. A system excited by only one force and returning n_s outputs is considered here for simplicity, the generalization to the multi-force case being quite straightforward. Thus, the input–output relation in a frequency band is

$$\mathbf{Y}(\omega) = \mathbf{H}(\omega)F(\omega) + \mathbf{N}(\omega), \quad \omega_l \le \omega \le \omega_u \tag{1}$$

with $\mathbf{Y}(\omega) \in \mathbb{C}^{n_s}$ the column vector of the n_s measured responses (e.g. accelerations) at frequency ω, $F(\omega) \in \mathbb{C}$ the force, $\mathbf{H}(\omega) \in \mathbb{C}^{n_s}$ the vector of FRFs at frequency ω between the positions of the n_s measured outputs and the position of the force, and $\mathbf{N}(\omega) \in \mathbb{C}^{n_s}$ the vector of the measurement noises. For a linear time-invariant system, the k-th generic element in the vector of $\mathbf{H}(\omega)$ is expressed as

$$H_k(\omega;\boldsymbol{\alpha}) = \sum_{r=1}^{m} \frac{-\omega^2 \mathcal{A}_{rk}}{\omega_r^2 - \omega^2 + 2\jmath\omega_r\omega\xi_r}, \tag{2}$$

where $\jmath = \sqrt{-1}$ and where the natural frequencies $\{\omega_r, r = 1,\ldots,m\}$, the damping ratios $\{\xi_r, r = 1,\ldots,m\}$ and all the modal residues $\{\mathcal{A}_{rk}, r = 1,\ldots,m; k = 1,\ldots,n_s\}$ are concatenated in vector $\boldsymbol{\alpha}$. The values of the modal parameters are typically returned by an updated FE model or experimental modal analysis; however, this is always to a limited degree of accuracy due to modeling or experimental errors and the fact that the real system is always more or less nonlinear. As a result, an additional term should be added in Eq. (1) to include explicitly the model uncertainty (nonlinear distortions, systematic error) in addition to measurement noise, which will be discussed later.

As emphasized in the Introduction, the Bayesian approach allows for the propagation and quantification of the errors on the reconstructed force by delivering a posterior probability distribution. Denoting by $\mathbf{x}$ the vector collecting the unknown parameters (force + measurement noise + model uncertainty), its joint posterior p.d.f. is obtained from Bayes' rule as

$$p(\mathbf{x}|\mathcal{D}) = p([Y]|\mathbf{x})p(\mathbf{x}|\mathcal{I})/p(\mathcal{D}), \tag{3}$$

where the matrix $[Y] \in \mathbb{C}^{n_\omega \times n_s}$ collects the n_s measured outputs at n_ω discrete frequencies in the frequency band of interest $[\omega_l, \omega_u]$, $\mathcal{I}$ is introduced to make explicit the prior information, and $\mathcal{D}$ is the union set of the prior information $\mathcal{I}$ and experimental information $[Y]$. The elements in Eq. (3) are listed as follows:

- the so-called likelihood function, $p([Y]|\mathbf{x})$, which reflects the probability of observing the data $[Y]$ given a set of parameters $\mathbf{x}$;
- the prior p.d.f., $p(\mathbf{x}|\mathcal{I})$, which reflects our knowledge on the parameters before experiments are undertaken. If $\mathbf{x}$ is well known, it is represented by a narrow p.d.f., otherwise by a flat one;

- the evidence function $p(\mathcal{D}) = \int p([Y]|\mathbf{x})p(\mathbf{x}|\mathcal{I})\,\mathrm{d}\mathbf{x}$, which is usually used for the model class selection and is independent of the model parameters.

The construction of the likelihood implies two steps, one is the characterization of the measurement noise, the other is the representation of the model uncertainty. According to the central limit theorem, the measurement noise in the frequency domain is asymptotically a zero-mean circular normal complex random variable with independent values over frequency [18,19]. The circular normal complex distribution $\mathcal{N}_c$ is illustrated in Appendix A. For instance, the measurement noise related to the k-th response,

$$N_k(\omega) \sim \mathcal{N}_c(0,\sigma_N^2) \tag{4}$$

with σ_N^2 an unknown hyper-parameter to be determined later (symbol $\sim$ means "distributed as"). The description of the model uncertainty and its consideration are vital for the model based force reconstruction. In the following sections this is formulated at two different levels: (a) at the level of FRFs when the uncertainty can be considered small over frequency, and (b) at the level of modal parameters when the uncertainty is significant in a certain frequency band.

3. Force reconstruction with uncertain FRFs

This section encodes the uncertainty of the forward model at the FRF's level. Assume the FRF ($\mathbf{H}(\omega)$) is biased from the underlying true FRF by a stochastic perturbation term; then the measured response reads

$$\mathbf{Y}(\omega) = \mathbf{H}(\omega)F(\omega) + \delta_{\mathbf{H}}(\omega)F(\omega) + \mathbf{N}(\omega), \tag{5}$$

where the perturbation $\delta_{\mathbf{H}}(\omega)$ represents the model uncertainty, and $\delta_{\mathbf{H}}(\omega)\mathbf{F}(\omega)$ is the uncertainty propagated to the response from the uncertain FRF. A rough assumption on the uncertainty $\delta_{\mathbf{H}}(\omega)\mathbf{F}(\omega)$ will be made in the next section so that it could be taken into account to some extent for force reconstruction.

3.1. Likelihood function and prior probability density function

In the case where the uncertainty $\delta_{\mathbf{H}}(\omega)\mathbf{F}(\omega)$ which is propagated to the response is assumed small enough, it may reasonably be included in the measurement noise $N_k(\omega)$ without changing its p.d.f., but only inflating the variance σ_N^2. Thus, the likelihood function simply reads

$$p([Y]|\mathbf{F},\sigma_N^{-2}) = \prod_{k=1}^{n_s} p(\mathbf{Y}_k|\mathbf{F},\sigma_N^{-2}), \tag{6}$$

where $p(\mathbf{Y}_k|\mathbf{F},\sigma_N^{-2}) \propto \sigma_N^{-2n_\omega}\exp(-(\mathbf{Y}_k - \lceil H_k \rfloor \mathbf{F})^*(\mathbf{Y}_k - \lceil H_k \rfloor \mathbf{F})/\sigma_N^2)$ (the superscript $*$ stands for the transpose conjugate operator), the diagonal matrix $\lceil H_k \rfloor = \mathrm{diag}(H_k(\omega_1),\ldots,H_k(\omega_{n_\omega}))$ and the column vector $\mathbf{F} = (F(\omega_1),\ldots,F(\omega_{n_\omega}))^t$ with the superscript t denoting the transpose operator.

Next a conjugate prior[1] is attributed to the force frequency components, i.e.,

$$\mathbf{F} \sim \mathcal{N}_c(\mathbf{F}_0, \lceil C_{F_0} \rfloor) \tag{7}$$

with $\mathbf{F}_0$ the vector of mean values and the diagonal covariance matrix $\lceil C_{F_0} \rfloor = \mathrm{diag}(\sigma_{F_0}^2(\omega_1),\ldots,\sigma_{F_0}^2(\omega_{n_\omega}))$ which are both frequency-dependent. The unknown hyper-parameters σ_N^2, $\mathbf{F}_0$, and $\lceil C_{F_0} \rfloor$ that come with the Bayesian approach are viewed as additional random variables to be inferred in vector $\mathbf{x}$. As such, they are also assigned priors in the form of conjugate distributions, i.e.,

$$\begin{aligned} \sigma_N^{-2} &\sim \Gamma(k_N,\beta_N), \\ F_0(\omega_i) &\sim \mathcal{N}_c(U_0,\sigma_{U_0}^2), \quad \forall i = 1,\ldots,n_\omega, \\ \sigma_{F_0}^{-2}(\omega_i) &\sim \Gamma(k_F,\beta_F), \quad \forall i = 1,\ldots,n_\omega, \end{aligned} \tag{8}$$

where $\Gamma(k,\beta)$ stands for the Gamma distribution[2] with shape and inverse scale parameters, and $\{U_0,\sigma_{U_0}^2\}$ are assumed to be independent of frequency. This is a so-called hierarchical Bayes model. The hierarchical relationship between the (hyper-) parameters is illustrated in Fig. 1. The hyper-parameters $\{k_N,\beta_N,k_F,\beta_F,U_0,\sigma_{U_0}^2\}$ appearing in the last hierarchical level in Eq. (8) are assumed known and constitute part of the prior information $\mathcal{I}$.

It should be remarked that the assumed prior p.d.f. might by no means be exact, even subjectively, since referring to quantities which are unknown by definition; its role is just to reflect some limited information available to the experimenter. However, such limited information is fundamental to deal with any underdetermination inherent to the inverse problem (e.g. non-identifiability, instable convergence). In addition, the defined prior p.d.f. is sometimes intended

[1] A conjugate prior is in the same p.d.f. family as the posterior.

[2] A Gamma distribution of a real-valued random variable x with shape and inverse scale parameters (k,β) has expression $p(x|k,\beta) = (\beta^k/(k-1)!)x^{k-1}\exp(-\beta x)$.

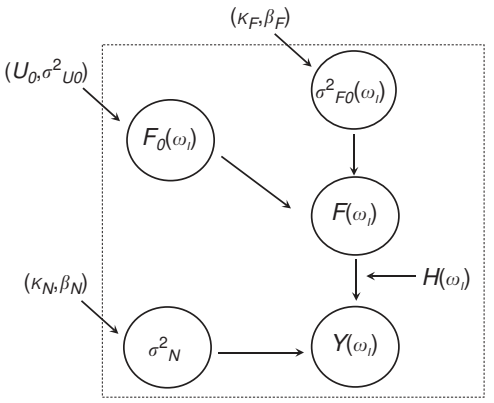

Fig. 1. The hierarchical Bayesian model of three stages: data model defined in Eq. (6), force model in Eq. (7) and parameter model in Eq. (8).

to have some specific forms (e.g. conjugate prior) to make easy subsequent Bayesian learning along with MCMC. Whatever the form of the assumed prior p.d.f. takes, it should cover all the possible values of the parameters, otherwise, a systematic error would occur. An important phenomenon to remind is that the likelihood function becomes more and more dominant when increasing experimental data, letting the truth gradually speak. This is well the case in the structural dynamics where a huge amount of data is often available.

3.2. Joint posterior probability distribution and local regularization

Given the prior p.d.f.'s in Eqs. (7) and (8) for the unknowns $\mathbf{F}$, $\mathbf{F}_0$, σ_N^2 and $\lceil C_{F_0}^{-1} \rfloor$, and putting all the unknowns on the left side of Bayes' rule, the application of Eq. (3) yields

$$p(\mathbf{F},\sigma_N^{-2},\mathbf{F}_0,\lceil C_{F_0}^{-1}\rfloor|\mathcal{D}) \propto p([Y]|\mathbf{F},\sigma_N^{-2})p(\mathbf{F}|\mathbf{F}_0,\lceil C_{F_0}^{-1}\rfloor)p(\mathbf{F}_0,\lceil C_{F_0}^{-1}\rfloor,\sigma_N^{-2}|\mathcal{I}). \tag{9}$$

The maximization of this posterior p.d.f. with respect to the force $\mathbf{F}$ then yields the posterior maximum estimator,

$$\hat{\mathbf{F}} = \left(\sum_{k=1}^{n_s} \lceil H_k \rfloor^* \lceil H_k \rfloor + \sigma_N^2 \lceil C_{F_0}^{-1} \rfloor \right)^{-1} \left(\sum_{k=1}^{n_s} \lceil H_k \rfloor^* \mathbf{Y}_k + \sigma_N^2 \lceil C_{F_0}^{-1} \rfloor \mathbf{F}_0 \right). \tag{10}$$

To establish a link with the classical regularization method, the standard Tikhonov approach is applied to reconstruct the force as the solution to the minimum penalized mean-squared error [20]

$$\sum_{i=1}^{n_\omega} (\|\mathbf{Y}(\omega_i) - \mathbf{H}(\omega_i)F(\omega_i)\|_2^2 + \lambda \|F(\omega_i) - F_0(\omega_i)\|_2^2), \tag{11}$$

where λ is called the regularization parameter, usually determined via the L-curve. The Tikhonov solution of the force is of the following form:

$$\mathbf{F}_{\text{tik}} = \left(\sum_{k=1}^{n_s} \lceil H_k \rfloor^* \lceil H_k \rfloor + \lambda \lceil I \rfloor \right)^{-1} \left(\sum_{k=1}^{n_s} \lceil H_k \rfloor^* \mathbf{Y}_k + \lambda \mathbf{F}_0 \right), \tag{12}$$

where $\lceil I \rfloor$ is an identity matrix of $n_\omega \times n_\omega$. By a straightforward comparison of Eqs. (10) and (12), it is found that the Tikhonov solution with a L_2 norm penalized term corresponds to the Bayesian solution with a normal prior distribution. More than a single optimal solution, the Bayesian approach also provides the uncertainty associated with the optimum. Equivalent to the parameter λ, the ratio $\sigma_N^2 \lceil C_{F_0}^{-1} \rfloor$ plays the role of a regularization parameter in the Tikhonov's sense to achieve a stable reconstruction. Another definite advantage of the Bayesian approach is that it will make possible the automatic tuning of its implicit regularization mechanism, as is described next. To make identifiable the frequency dependent regularization parameter in the Bayesian case, the whole frequency band is divided into n_e segments D_l, in each of which the force spectra are considered to have almost constant mean value and variance, i.e.,

$$F_0(\omega_i) \simeq F_0(l), \quad \lceil C_{F_0}(\omega_i) \rfloor \simeq \sigma_{F_0}^2(l), \ \forall i \in D_l, \ l = 1, \ldots n_e. \tag{13}$$

This returns a piece-wise constant regularization parameter $\{\sigma_N^2/\sigma_{F_0}^2(l), l = 1, \ldots, n_e\}$ well suited to situations where the force variance cannot be assumed constant over the whole frequency band. The segmentation of the frequency band can be investigated as a problem of model selection, which is not discussed in this work.

The posterior p.d.f. in Eq. (9) returns the complete updated information of all the parameters to be inferred. In the following section, a Monte Carlo Markov chain method is implemented to extract the improved knowledge by simulating samples from this joint probability distribution. Then the force and the parameters of regularization are simultaneously estimated by averaging these samples or finding a sample which maximizes the posterior probability.

3.3. MCMC implementation

The principle of MCMC essentially consists in generating random walks whose stationary p.d.f. coincides with the posterior p.d.f. of interest. Among the MCMC methods [21–23], the Gibbs sampling algorithm initiated in [22] is used to explore the posterior p.d.f. in Eq. (9) due to the fact that all the conditional p.d.f.'s are usual distributions, from which random variables can be easily generated. The implementation of the Gibbs sampling on force reconstruction is resumed as follows (See Appendix B for details on how to derive these equations).

Algorithm 1.

1. initialize the values of $\mathbf{F}_0$, σ_N^2 and $\lceil C_{F_0}^{-1} \rfloor$ from their prior p.d.f.'s.
2. draw $\mathbf{F}|\mathbf{F}_0, \lceil C_{F_0}^{-1} \rfloor, \sigma_N^{-2}, \mathcal{D} \sim \mathcal{N}_c(\hat{\mathbf{F}}, \lceil \hat{C}_F \rfloor)$ with
   $\lceil \hat{C}_F \rfloor = \left(\sum_{k=1}^{n_s} \lceil H_k \rfloor^* \lceil H_k \rfloor \sigma_N^{-2} + \lceil C_{F_0}^{-1} \rfloor \right)^{-1}$,
   $\hat{\mathbf{F}} = \lceil \hat{C}_F \rfloor \left(\sum_{k=1}^{n_s} \lceil H_k \rfloor^* \mathbf{Y}_k / \sigma_N^2 + \lceil C_{F_0}^{-1} \rfloor \mathbf{F}_0 \right)$.
3. $\sigma_N^{-2}|\mathbf{F}, \mathcal{D} \sim \Gamma(\hat{k}_N, \hat{\beta}_N)$ with
   $\hat{k}_N = k_N + n_\omega n_s$,
   $\hat{\beta}_N = \beta_N + \sum_{k=1}^{n_s} (\mathbf{Y}_k - \lceil H_k \rfloor \mathbf{F})^* (\mathbf{Y}_k - \lceil H_k \rfloor \mathbf{F})$.
4. draw $\sigma_{F_0(l)}^{-2} | \mathbf{F}, \mathbf{F}_0 \sim \Gamma(\hat{k}_F, \hat{\beta}_F)$ with
   $\hat{k}_F = k_F + |D_l|$,
   $\hat{\beta}_F = \beta_F + \sum_{i \in D_l} (F(\omega_i) - F_0(l))^* (F(\omega_i) - F_0(l))$ ($|D_l|$ is the number of frequencies in the l-th segment).
5. draw $F_0(l)|\mathbf{F}, \lceil C_{F_0}^{-1} \rfloor \sim \mathcal{N}(\hat{U}_0, \hat{\sigma}_{U_0}^2)$ with
   $\hat{\sigma}_{U_0}^2 = (|D_l| \sigma_{F_0(l)}^{-2} + \sigma_{U_0}^{-2})^{-1}$,
   $\hat{U}_0 = \left(\sigma_{F_0(l)}^{-2} \sum_{i \in D_l} F(\omega_i) + U_0 \sigma_{U_0}^{-2} \right) \hat{\sigma}_{U_0}^2$.
6. go to step 2 and repeat until a sufficiently large sample is collected after the burn-in phrase.

The Markov chain needs a heating stage to attain the convergence towards the target p.d.f.; this stage is the so-called burn-in phrase, in which the samples are not yet drawn from the target probability distribution. The convergence of a Markov chain can be roughly verified by inspecting its trajectory, or more reliably by several repetition of simulated Markov chains that should converge to the same probability distribution. Integrated within the above MCMC sampling scheme, the proposed Bayesian approach is capable of dealing with the general force reconstruction problem based on an uncertain model. However, it is worth noting that because accelerometers do not pass the DC component, the mean value of the temporal force is in theory impossible to reconstruct unless strong prior information is available; for instance, if the force spectrum is known to be relatively flat, then its value at the zero frequency can be estimated by extrapolation.

3.4. Marginal posterior probability distribution of the force

To have a reliable reconstruction is a major objective of the indirect force measurement. From the Bayesian perspective, the information of the reconstructed force is indeed completely described by its marginal posterior p.d.f. which is also called the predictive distribution. It is by definition the expectation of the p.d.f. $p(\mathbf{F}|\mathbf{F}_0, \lceil C_{F_0}^{-1} \rfloor, \sigma_N^{-2}, \mathcal{D})$ with respect to the p.d.f. $p(\mathbf{F}_0, \lceil C_{F_0}^{-1} \rfloor, \sigma_N^{-2}|\mathcal{D})$. By the strong law of large numbers, this expectation can be asymptotically approximated by averaging $p(\mathbf{F}|\mathbf{F}_0, \lceil C_{F_0}^{-1} \rfloor, \sigma_N^{-2}, \mathcal{D})$ over the samples $\{\mathbf{F}_0(i), \lceil C_{F_0}^{-1}(i) \rfloor, \sigma_N^{-2}(i), i = 1, \ldots, n\}$ returned by the Gibbs sampling algorithm. This procedure is stated in the following equation:

$$p(\mathbf{F}|\mathcal{D}) = \int p(\mathbf{F}, \mathbf{F}_0, \left\lceil C_{F_0}^{-1} \right\rfloor, \sigma_N^2 | \mathcal{D}) \, \mathrm{d}\mathbf{F}_0 \mathrm{d}\sigma_N^{-2} \mathrm{d} \left\lceil C_{F_0}^{-1} \right\rfloor = \int p(\mathbf{F}|\mathbf{F}_0, \left\lceil C_{F_0}^{-1} \right\rfloor, \sigma_N^{-2}, \mathcal{D}) p(\mathbf{F}_0, \left\lceil C_{F_0}^{-1} \right\rfloor, \sigma_N^{-2} | \mathcal{D}) \, \mathrm{d}\mathbf{F}_0 \mathrm{d}\sigma_N^{-2} \mathrm{d} \left\lceil C_{F_0}^{-1} \right\rfloor$$
$$\approx \frac{1}{n} \sum_{i=1}^{n} p(\mathbf{F}|\mathbf{F}_0(i), \left\lceil C_{F_0}^{-1}(i) \right\rfloor, \sigma_N^{-2}(i), \mathcal{D}). \tag{14}$$

As stated in Step 2 of Algorithm 1, $p(\mathbf{F}|\mathbf{F}_0, \lceil C_{F_0}^{-1} \rfloor, \sigma_N^{-2}, \mathcal{D})$ is a circular complex normal distribution of diagonal covariance matrix; $p(\mathbf{F}|\mathcal{D})$ is then approximated as a mixture of these distributions. The posterior p.d.f. of the reconstructed force at each frequency, $p(F(\omega)|\mathcal{D})$, can be easily evaluated based on a 2-D grid formed by its real and imaginary parts. In turn, the marginal p.d.f.'s of the real and imaginary parts are found as

$$p(\mathrm{Re}(F(\omega))|\mathcal{D}) = \int p(F(\omega)|\mathcal{D}) \, \mathrm{d} \, \mathrm{Im}(F(\omega)),$$

$$p(\mathrm{Im}(F(\omega))|\mathcal{D}) = \int p(F(\omega)|\mathcal{D}) \, \mathrm{d} \, \mathrm{Re}(F(\omega)), \tag{15}$$

where Re(·) and Im(·) stand for real and imaginary parts. Since these two marginal p.d.f.'s may be asymmetrical, the Bayesian credible interval is used in practice to describe the uncertainty associated with the reconstructed force, i.e., all the confidence intervals with an user-chosen level are calculated for each frequency, and the shortest one is chosen among them [24].

4. Force reconstruction with uncertain modal parameters

In some cases, the FRFs returned by a (even updated) FE model still have so considerable error in certain frequency bands that it jeopardizes the former force reconstruction strategy. This is because the modeling error, if much greater than the measurement noise, can no longer be approximated as independent and identically distributed with respect to frequency. In this section, uncertainty is introduced at the level of the modal parameters instead of the FRFs in order to correctly reproduce a modeling error whose magnitude depends on frequency – e.g. greater on resonances – and whose values are dependent across frequencies. An algorithm is then proposed to jointly correct it together with the force reconstruction.

4.1. Joint approach for force reconstruction and model updating

The uncertainty of the model is described here by assigning a p.d.f. $p(\boldsymbol{\alpha})$ to the modal parameters in a given frequency band. According to Bayes' rule, the joint p.d.f. of the force, modal parameter and variance of measurement noise is

$$p(\mathbf{F},\boldsymbol{\alpha},\sigma_N^{-2}|\mathcal{D}) \propto p([Y]|\mathbf{F},\boldsymbol{\alpha},\sigma_N^{-2})p(\mathbf{F},\boldsymbol{\alpha},\sigma_N^{-2}|\mathcal{I}). \tag{16}$$

However, this joint approach which involves more parameters to identify possibly leads to a non-identifiable problem since the force and the uncertain modal parameters are functionally dependent and thus non-separable given the measurements. For instance, there is clearly an arbitrary scaling factor κ such that $\kappa\mathbf{F}$ and $\kappa^{-1}\lceil H(\boldsymbol{\alpha})\rfloor$ are equivalently valid solutions of the problem. In order to solve this non-identifiability issue, one possible way is to introduce extra prior information about the force spectrum. This may be achieved by expanding the unknown force spectrum onto a relevant basis that can capture its behavior with few components. For instance, an impulsive force will be well described by a few very smooth basis functions in the frequency domain, and a periodic force by a few delta impulses. By introducing such constraints – which is equivalent to decreasing the number of unknowns of the problem – the non-identifiability problem can thus be solved in an implicit way. More specifically, let us expand the unknown force as

$$\mathbf{F} = [B]\mathbf{X} + \boldsymbol{\eta}, \tag{17}$$

where $B \in \mathbb{R}^{n_\omega \times n_X}$ is the matrix of suitably chosen basis functions, n_X the number of the basis functions, $\mathbf{X} \in \mathbb{C}^{n_X}$ the vector of complex coefficients, and $\boldsymbol{\eta}$ a vector of residual errors which are assumed to follow a zero-mean circular complex normal p.d.f. with unknown variance σ_η^2. The number of the basis functions is assumed known *a priori*. One can approximately select the number of the basis function in some cases from the available information on the force to be reconstructed. In fact, it can be systematically addressed by means of the technique called model order selection, for which the Bayesian approach provides unique solutions: the number of the basis function is determined by finding an optimal compromise between the term of good-fitness and the penalized term [25].

Within the Bayesian framework the reconstruction problem then amounts to finding the joint posterior

$$p(\mathbf{F},\mathbf{X},\boldsymbol{\alpha},\sigma_N^{-2},\sigma_\eta^{-2}|\mathcal{D}) \propto p([Y]|\mathbf{F},\boldsymbol{\alpha},\sigma_N^{-2})p(\mathbf{F}|\mathbf{X},\sigma_\eta^{-2})p(\mathbf{X},\boldsymbol{\alpha},\sigma_\eta^{-2},\sigma_N^{-2}|\mathcal{I}), \tag{18}$$

where the likelihood function $p([Y]|\mathbf{F},\boldsymbol{\alpha},\sigma_N^2)$ is defined similarly as Eq. (6) except that the FRF is a function of $\boldsymbol{\alpha}$, the prior p.d.f. $p(\mathbf{F}|\mathbf{X},\sigma_\eta^{-2}) = \mathcal{N}_c([B]\mathbf{X},\sigma_\eta^2\lceil I\rfloor)$ with $\lceil I\rfloor$ the identity matrix, and $\{\mathbf{X},\boldsymbol{\alpha},\sigma_\eta^{-2},\sigma_N^{-2}|\mathcal{I}\}$ are independent in a prior view. In order to reflect our complete state of ignorance, an uniform distribution is chosen for $p(\mathbf{X})$, and conjugate Gamma p.d.f.'s are assigned to σ_η^{-2} and σ_N^{-2} as defined in Eq. (8).

4.2. Gibbs sampling coupled with Metropolis–Hastings algorithm

All the conditional p.d.f.'s in the right-hand-side of Eq. (18) are usual p.d.f.'s except that of the modal parameters, $p(\boldsymbol{\alpha}|\mathbf{F},\sigma_N^{-2},\mathcal{D})$. Therefore a sampling method based on Gibbs sampling coupled with Metropolis–Hastings algorithm [21,26] is adopted here to explore the joint posterior probability distribution.

Algorithm 2.

1. initialize $\mathbf{X}$, $\boldsymbol{\alpha}$, σ_N^{-2}, σ_η^{-2} from their prior p.d.f.'s.
2. draw $\mathbf{F}|\boldsymbol{\alpha},\mathbf{X},\sigma_N^{-2},\sigma_\eta^{-2},\mathcal{D} \sim \mathcal{N}_c(\hat{\mathbf{F}},\lceil\hat{C}_F\rfloor)$ where
$$\lceil\hat{C}_F\rfloor = \left(\sum_{k=1}^{n_s} \lceil H_k(\boldsymbol{\alpha})\rfloor^* \lceil H_k(\boldsymbol{\alpha})\rfloor \sigma_N^{-2} + \sigma_\eta^{-2}\lceil I\rfloor\right)^{-1},$$
$$\hat{\mathbf{F}} = \lceil\hat{C}_F\rfloor\left(\sum_{k=1}^{n_s} \sigma_N^{-2}\lceil H_k(\boldsymbol{\alpha})\rfloor^*\mathbf{Y}_k + \sigma_\eta^{-2}[B]\mathbf{X}\right).$$
3. draw $\mathbf{X}|\boldsymbol{\alpha},\sigma_\eta^{-2},\sigma_N^{-2},\mathcal{D} \sim \mathcal{N}_c(\hat{\mathbf{X}},[\hat{C}_X])$ where

$[\hat{C}_X] = ([B]^* \lceil H_s(\boldsymbol{\alpha}) \rfloor^* (\lceil H_s(\boldsymbol{\alpha}) \rfloor^* \lceil H_s(\boldsymbol{\alpha}) \rfloor \sigma_\eta^2 + \sigma_N^2)^{-1} \lceil H_s(\boldsymbol{\alpha}) \rfloor [B])^{-1}$,

$\hat{\mathbf{X}} = [\hat{C}_X][B]^* (\lceil H_s(\boldsymbol{\alpha}) \rfloor^* \lceil H_s(\boldsymbol{\alpha}) \rfloor \sigma_\eta^2 + \sigma_N^2)^{-1} \sum_{k=1}^{n_s} \lceil H_k(\boldsymbol{\alpha}) \rfloor^* \mathbf{Y}_k$

with $\lceil H_s(\boldsymbol{\alpha}) \rfloor = \sqrt{\sum_{k=1}^{n_s} \lceil H_k(\boldsymbol{\alpha}) \rfloor^* \lceil H_k(\boldsymbol{\alpha}) \rfloor}$.

4. draw $\sigma_\eta^{-2} | \mathbf{F}, \mathbf{X} \sim \Gamma(\hat{k}_\eta, \hat{\beta}_\eta)$ with
   $\hat{k}_\eta = k_\eta + n_\omega$, $\hat{\beta}_\eta = \beta_\eta + (\mathbf{F} - [B]\mathbf{X})^* (\mathbf{F} - [B]\mathbf{X})$.
5. draw $\sigma_N^{-2} | \mathbf{F}, \boldsymbol{\alpha}, \mathcal{D} \sim \Gamma(\hat{k}_N, \hat{\beta}_N)$ with
   $\hat{k}_N = k_N + n_\omega n_s$, $\hat{\beta}_N = \beta_N + \sum_{k=1}^{n_s} (\mathbf{Y}_k - \lceil H_k(\boldsymbol{\alpha}) \rfloor \mathbf{F})^* (\mathbf{Y}_k - \lceil H_k(\boldsymbol{\alpha}) \rfloor \mathbf{F})$.
6. draw $\boldsymbol{\alpha} \sim p(\boldsymbol{\alpha} | \mathbf{F}, \sigma_N^{-2}, \mathcal{D})$ using the Metropolis–Hastings algorithm.
7. go to Step 2 until a sufficiently large sample is collected after the convergence of Markov chains.

The conditional p.d.f. of $\mathbf{X}$ and the Metropolis–Hastings algorithm (Step 6 of Algorithm 2) are detailed in Appendix C.

4.3. Posterior probability distribution of the reconstructed force

The proposed joint approach along with the MCMC sampling scheme described above estimates the unknown parameters in an iterative way: the force is simultaneously reconstructed with the feasible update of the uncertain modal in each loop. Similar to the case in Section 3.4, the posterior model uncertainty and the qualified errors are also taken into account to obtain a full reconstruction. By definition, the marginal posterior p.d.f. of the force reads

$$p(\mathbf{F} | \mathcal{D}) = \int p(\mathbf{F}, \mathbf{X}, \boldsymbol{\alpha}, \sigma_N^2, \sigma_\eta^{-2}) \, \mathrm{d}\mathbf{X} \, \mathrm{d}\boldsymbol{\alpha} \, \mathrm{d}\sigma_N^2 \, \mathrm{d}\sigma_\eta^{-2}. \tag{19}$$

In accordance with the force model (17), Eq. (19) is factorized into

$$\begin{aligned} p(\mathbf{F} | \mathcal{D}) &= \int p(\mathbf{F} | \mathbf{X}, \sigma_\eta^{-2}) p(\mathbf{X}, \boldsymbol{\alpha}, \sigma_N^2, \sigma_\eta^{-2} | \mathcal{D}) \, \mathrm{d}\mathbf{X} \, \mathrm{d}\boldsymbol{\alpha} \, \mathrm{d}\sigma_N^2 \, \mathrm{d}\sigma_\eta^{-2} = \int p(\mathbf{F} | \mathbf{X}, \sigma_\eta^{-2}) p(\mathbf{X} | \boldsymbol{\alpha}, \sigma_N^2, \sigma_\eta^{-2}, \mathcal{D}) p(\boldsymbol{\alpha}, \sigma_N^2, \sigma_\eta^{-2} | \mathcal{D}) \, \mathrm{d}\mathbf{X} \, \mathrm{d}\boldsymbol{\alpha} \, \mathrm{d}\sigma_N^2 \, \mathrm{d}\sigma_\eta^{-2} \\ &\approx \frac{1}{n} \sum_{i=1}^{n} \int p(\mathbf{F} | \mathbf{X}, \sigma_\eta^{-2}(i)) p(\mathbf{X} | \boldsymbol{\alpha}(i), \sigma_N^2(i), \sigma_\eta^{-2}(i), \mathcal{D}) \, \mathrm{d}\mathbf{X} = \frac{1}{n} \sum_{i=1}^{n} \mathcal{N}_c(\hat{\mathbf{F}}(i), [\hat{C}_F(i)]), \end{aligned} \tag{20}$$

where $\hat{\mathbf{F}}(i) = [B]\hat{\mathbf{X}}(i)$, $[\hat{C}_F(i)] = [B][\hat{C}_X(i)][B]^* + \lceil I \rfloor \sigma_\eta^2(i)$ with $\hat{\mathbf{X}}$ and $[\hat{C}_X]$ defined in Step 3 of Algorithm 2. It is shown that $p(\mathbf{F} | \mathcal{D})$ is an averaged p.d.f. over all the possible realization values ($n \to \infty$) of the modal model parameters, the qualified measurement and residue errors. Eq. (20) provides a full solution of the reconstructed force in the form of a mixture of multi-dimension complex normal p.d.f.'s over all the selected frequencies. As is well known, applying a marginalization step to a multi-dimension normal p.d.f. still returns a normal p.d.f of a reduced dimension. Hence, the posterior p.d.f. of the force at any frequency line can be analytically evaluated by a marginalization step. For instance, at the j-th frequency line,

$$p(F(\omega_j) | \mathcal{D}) = \frac{1}{n} \sum_{i=1}^{n} \int p(\mathbf{F} | \hat{\mathbf{F}}(i), \hat{C}_F(i), \mathcal{D}) \, \mathrm{d}\mathbf{F}(\omega_{[-j]}) = \frac{1}{n} \sum_{i=1}^{n} \mathcal{N}_c([B]_{[j]} \hat{\mathbf{X}}(i), \hat{\sigma}_{F,[j]}^2(i)), \tag{21}$$

where $[B]_{[j]}$ and $\hat{\sigma}_{F,[j]}^2$ are respectively the row of the matrix $[B]$ and the diagonal element of $[\hat{C}_F(i)]$ corresponding to frequency ω_j and the set $[-j]$ collects all the frequency indices except the j-th one. In the same way as stated in Section 3.4, the Bayesian credible intervals are finally built.

Finally, it is remarked that the application of the presented joint approach is limited by the choice of the basis functions. To alleviate this limitation, one feasible way is to combine the both approaches presented above: firstly update the uncertain model by applying certain kind of force of known characteristics (e.g. smooth form) using the joint approach, and then reconstruct any general force based on the updated model using the approach presented in Section 3. Another direction is to model the force for instance by Gaussian processes or high order Markov chains, which is quite general for force reconstruction. This will be addressed in future work.

5. Numerical and experimental applications

The proposed force reconstruction approaches are now illustrated on numerical and experimental examples.

5.1. Numerical example

The approach presented in Section 4 is used to reconstruct an impulsive-like force based on an uncertain modal model, such as returned for instance by a stochastic FE model. In this simulation case, an acceleration measurement is simulated by exciting the true model with an impulsive-like force and adding measurement noise with signal-to-noise ratio (SNR) of 78.5 dB, as illustrated in Fig. 2. The prior nominal model is built by adding 40 percent and 30 percent systematic errors

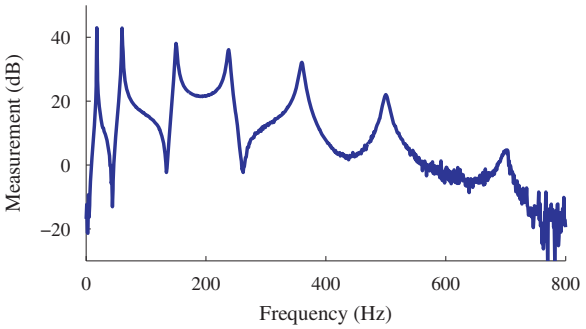

Fig. 2. Spectrum of simulated measurement.

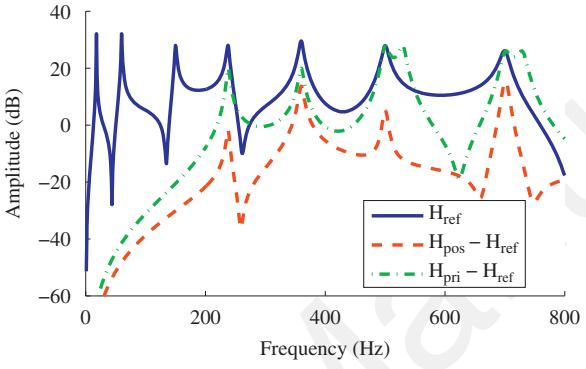

Fig. 3. Illustration of model update by comparing ($\mathbf{H}_{\text{pri}}-\mathbf{H}_{\text{ref}}$) and ($\mathbf{H}_{\text{pos}}-\mathbf{H}_{\text{ref}}$) ($\mathbf{H}_{\text{ref}}$: true FRF, $\mathbf{H}_{\text{pri}}$: prior nominal FRF, $\mathbf{H}_{\text{pos}}$: FRF with posterior means of the modal parameters).

to the modal residues of the 4th and 5th modes of the underlying true model, respectively and a 30 Hz deviation to the 6th and 7th natural frequencies of the true model. The underlying true FRF and the deviation of the prior nominal FRF from the true one are illustrated in Fig. 3. The former modal parameters (4th and 5th modal residues and 6th and 7th natural frequencies) are thus regarded as uncertain and assumed to follow a multi-variate normal distribution $\mathcal{N}(\boldsymbol{\alpha}_0,\lceil C_{\boldsymbol{\alpha}}\rfloor)$ with $\boldsymbol{\alpha}_0=[-0.7,-0.4,530,730]$ and covariance matrix $\lceil C_{\boldsymbol{\alpha}}\rfloor=\text{diag}(0.04,0.04,200,200)$. The matrix covariance is chosen large enough to cover all possible values of the uncertain modal parameters. This uncertain prior model will be used to reconstruct the unknown force from Bayesian inference.

By virtue of the spectral regularity of the force to reconstruct, 10 Legendre polynomials are used to build the basis matrix $[B]$ of Eq. (17); the prior information on the residual error (k_η,σ_η^2) and the measurement error (k_N,σ_N^2) is both set to (10,1).[3] The MCMC sampling Algorithm 2 is followed to draw $n=10^4$ samples from the joint p.d.f. in Eq. (18) and the first 10^3 are discarded to remove the burn-in phase. The posterior mean values of the force, say $\mathbf{F}_{\text{pos}}$, and of all uncertain modal parameters can then be estimated jointly from these samples. In turn, the posterior FRF ($\mathbf{H}_{\text{pos}}$) is computed using the posterior mean values of the updated modal parameters. Fig. 3 shows the residual error between the true FRF ($\mathbf{H}_{\text{ref}}$) and the updated one, which is much less than the prior nominal FRF ($\mathbf{H}_{\text{pri}}$). The quality of the update is clearly seen to depend on the SNR as a function of frequency. The posterior force ($\mathbf{f}_{\text{pos}}$) in the time domain is ultimately obtained from the inverse Fourier transform of the posterior mean value ($\mathbf{F}_{\text{pos}}$) and is compared with the reference force ($\mathbf{f}_{\text{ref}}$) in Fig. 4, showing an excellent overall agreement. The force is also reconstructed based on the prior nominal model, denoted by ($\mathbf{f}_{\text{pri}}$) which is less accurate on the peak and more oscillating in other parts.

Finally, 98 percent Bayesian credible intervals are constructed based on Eq. (20) for the real part and the imaginary part of the force, as shown in Figs. 5 and 6, respectively. It is seen that the reconstructed force based on the posterior model globally agree much better with the reference force than the reconstructed one based on the prior model. Incidentally, Figs. 7 and 8 display the histograms of σ_N^2 and σ_η^2 which gives a good sign that the sampling algorithm has converged.

5.2. Experimental example

This section illustrates the application of the proposed approach to reconstruct actual forces applied on a laboratory beam structure of low-carbon steel. The beam is clamped in a vise that is buried into tamped sand. The part of the beam

[3] Hierarchical Bayes is known to be very robust with respect to hyperparameters settings, which justifies this arbitrary choice [16].

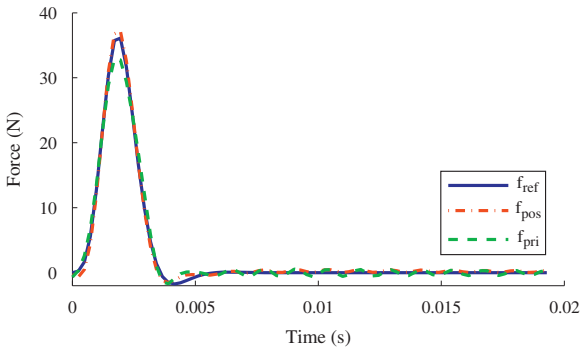

Fig. 4. Reconstructed force in time domain ($\mathbf{f}_{ref}$: reference force, $\mathbf{f}_{pri}$: force reconstructed based on the prior model, $\mathbf{f}_{pos}$: force reconstructed jointly with model updating).

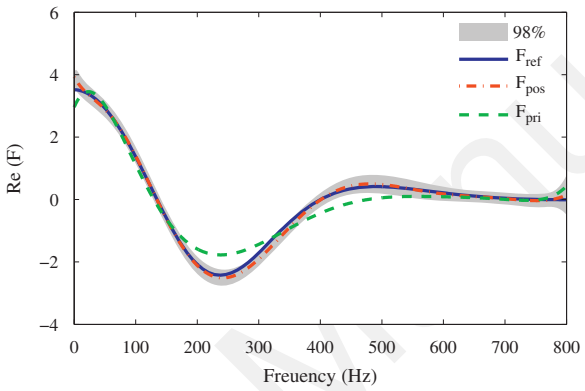

Fig. 5. Real part (gray zone: 98 percent credible interval, $\mathbf{F}_{ref}$: reference force, $\mathbf{F}_{pri}$: force reconstructed based on the prior model, $\mathbf{F}_{pos}$: force reconstructed jointly with model updating).

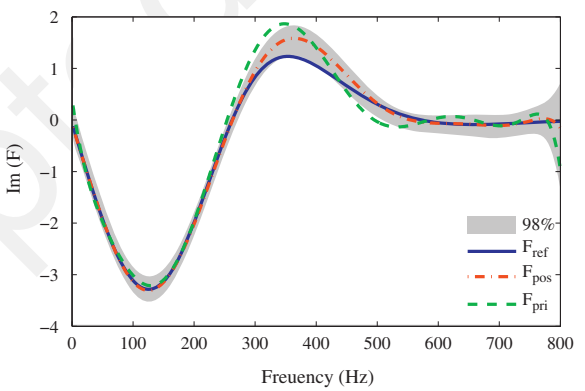

Fig. 6. Imaginary part (gray zone: 98 percent credible interval, $\mathbf{F}_{ref}$: reference force, $\mathbf{F}_{pri}$: force reconstructed based on the prior model, $\mathbf{F}_{pos}$: force reconstructed jointly with model updating).

out of the vise is of the dimension (length $\times$ width $\times$ thickness): $45 \times 3 \times 0.5$ cm. In a first stage, a controlled excitation is applied to the beam through a shaker and three acceleration transducers are used to measure the structural responses, as illustrated in Fig. 9. A beam-type FE model where the boundary condition is modeled by a rotational spring is then updated using these measurements [27].

Fig. 10 shows that the updated FRFs agree very well with the measured ones, to the exception of small discrepancies at the resonances. Besides, it is worth noting that the excitation system (mass of the impedance head) and the presence of accelerometers slightly modify the structure under test, whereas force reconstruction is actually based on the model of the beam structure alone. Such modifications of the structural configuration are likely to induce changes of the modal property, and will cause additional difficulties in the inversion step especially when the structure is lightly damped.

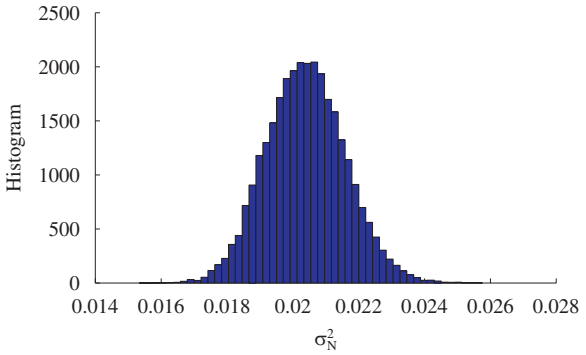

Fig. 7. Histogram of σ_N^2.

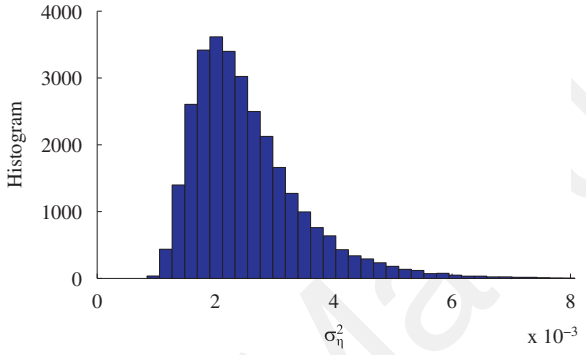

Fig. 8. Histogram of σ_η^2.

Fig. 9. Experimental plant.

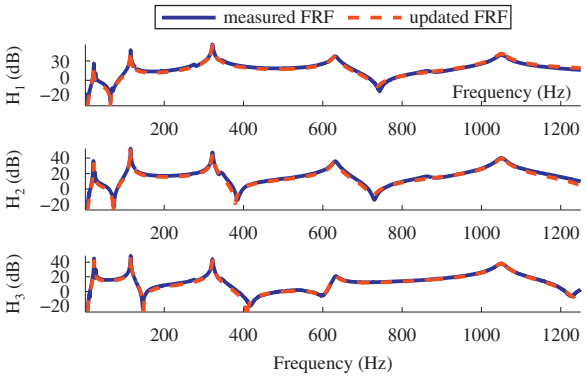

Fig. 10. Predicted FRFs based on the updated FE model.

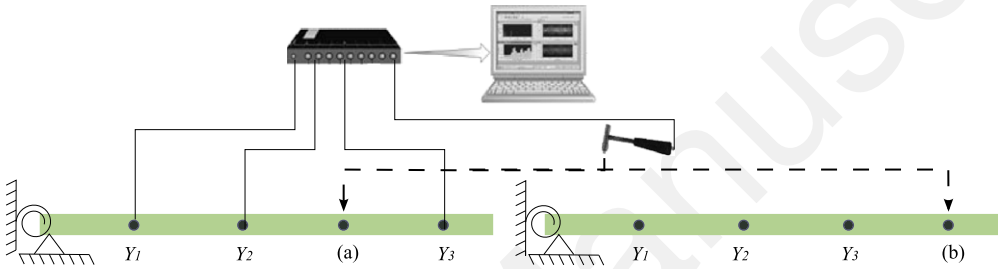

Fig. 11. Layout of the excitation and measurements.

In a second stage, the shaker is removed and two forces are exerted on the beam with a hammer equipped with tips of different hardness, and measured with an impedance head – the experimental layout is illustrated in Fig. 11:

- the first force is a single impact applied at the same location (a) as used to update the FE model,
- the second force is a series of impacts applied at a different location (b) which did not serve in the FE model updating.

All measurements are acquired with a sampling frequency $f_s = 5120$ Hz and the applied forces are simultaneously recorded to serve as references for the purpose of validation. In order to handle the aforementioned modification of the modal properties, the MCMC Algorithm 2 of Section 4 is used to refine the modal parameters and reconstruct the force as well as possible; 10 Legendre polynomials are used to build the basis matrix $[B]$ in accordance with the assumed regularity of the force spectrum at location (a).

5.2.1. Reconstruction of the single-impact force

In this example, the five natural frequencies in the frequency band of interest are chosen to be updated together with the force reconstruction. To have an effective correction of the natural frequencies, a partial updating scheme is used, e.g., the 1st and 2nd natural frequencies are firstly tuned, then the 3rd, 4th and 5th ones. For instance, Figs. 12 and 13 show the Markov chains of 3rd and 5th natural frequencies. The force transformed back to the time domain is compared with the measured one in Fig. 14, which shows excellent agreement.

In the same way as previously done in the numerical example, the joint p.d.f. of the force in Eq. (21) serves to construct the Bayesian credible intervals, such as illustrated in Fig. 15 at frequency 62.5 Hz. Figs. 16 and 17 show the 98 percent Bayesian credible intervals for the real and imaginary parts of the force that encapsulate both measurement and modeling errors.

5.2.2. Reconstruction of a multiple-impact force

In this example, a multiple-impact force applied at location (b) is reconstructed based on the updated modal parameters from the previous example. Three recorded measurements at the locations shown in Fig. 11 are displayed with their related FRFs in Fig. 18. They all evidence high SNRs, except possibly in the very low frequency band (< 10) Hz. As a consequence, the Bayesian MCMC Algorithm 1 of Section 3 is adopted here to reconstruct the force.

In order to account for the spectral non-stationary of the force, the whole frequency band is segmented equally into $n_e = 80$ elements. The hyper-parameters are set to $(k_N = 10, \beta_N = 1)$, $(k_F = 10, \beta_F = 0.1)$ and $(U_0 = 0, \sigma^2_{U_0} = 100)$. After running a MCMC, $n = 2 \times 10^4$ samples are drawn from the joint posterior p.d.f. of Eq. (9), and the mean values and the 98 percent

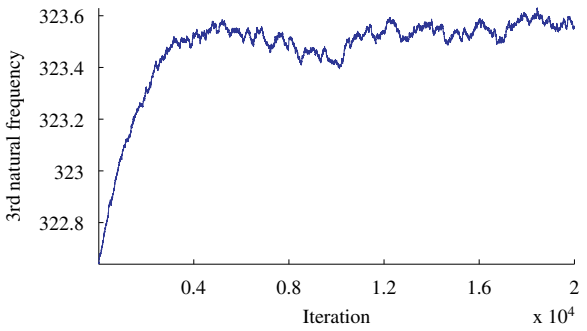

Fig. 12. Markov chain of 3rd natural frequency.

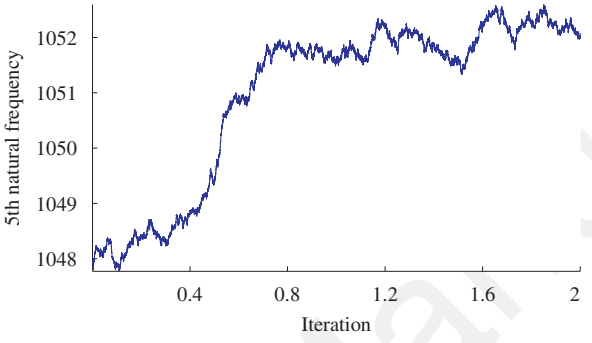

Fig. 13. Markov chain of 5th natural frequency.

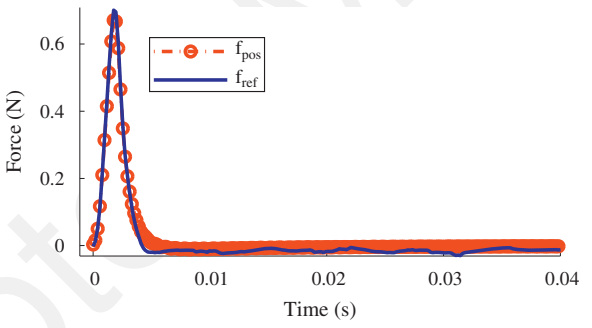

Fig. 14. Reconstructed force in time domain.

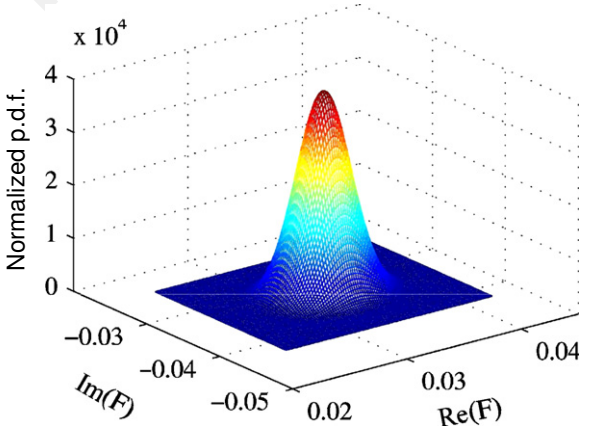

Fig. 15. Joint p.d.f. of the force at frequency 62.5 Hz.

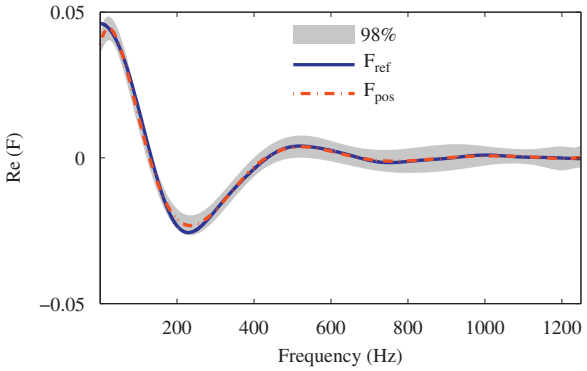

Fig. 16. Real part (gray zone: 98 percent credible interval, $\mathbf{F}_{\text{ref}}$: reference force, $\mathbf{F}_{\text{pos}}$: force reconstructed jointly with model updating).

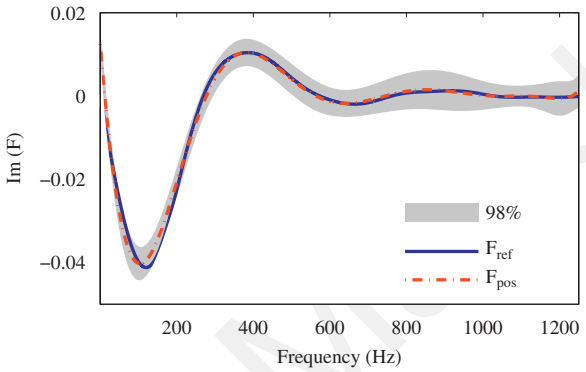

Fig. 17. Imaginary part (gray zone: 98 percent credible interval, $\mathbf{F}_{\text{ref}}$: reference force, $\mathbf{F}_{\text{pos}}$: force reconstructed jointly with model updating).

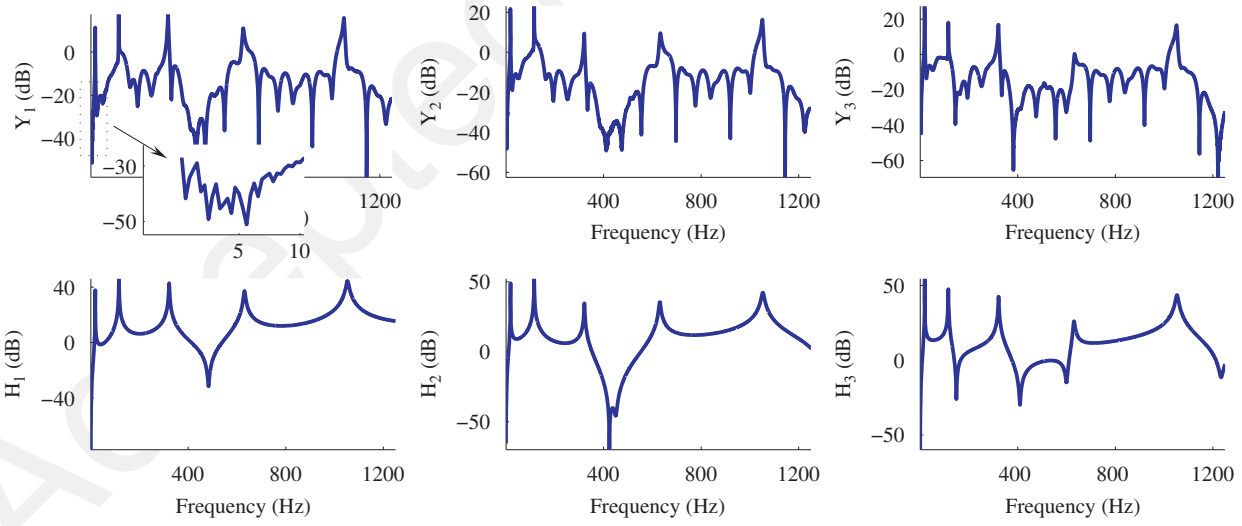

Fig. 18. Spectra of the measurements and related FRFs.

credible intervals at each frequency are constructed using the posterior mean of the parameters $\{\mathbf{F}_0, \sigma_N^2, \lceil C_{F_0} \rfloor\}$ according to Eq. (14), as displayed in Figs. 19 and 20. It is seen that the reconstructed force ($\mathbf{F}_{\text{pos}}$) matches very well the measured one ($\mathbf{F}_{\text{ref}}$), except in the frequency band [400, 500] Hz where the three FRFs all have deep anti-resonances – see Fig. 18 – and therefore hardly transmit information to the sensors. The reconstructed force consequently has a large uncertainty there, which could surely be improved by optimizing the placement of the transducers. But the important point is that the

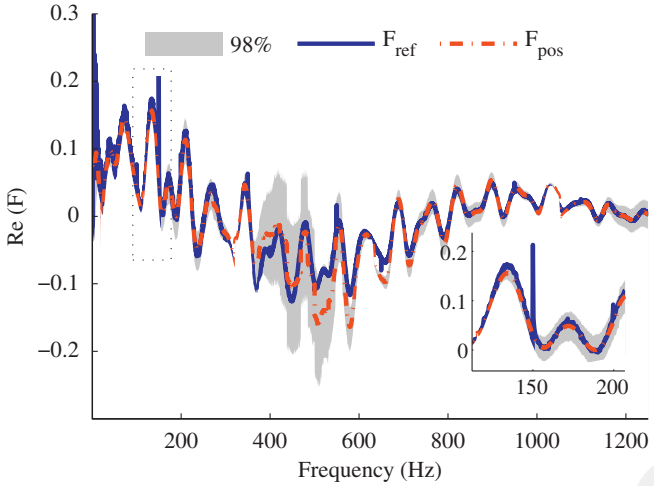

Fig. 19. Real part (gray zone: 98 percent credible interval, $\mathbf{F}_{ref}$: reference force, $\mathbf{F}_{pos}$: posterior mean value of reconstructed force).

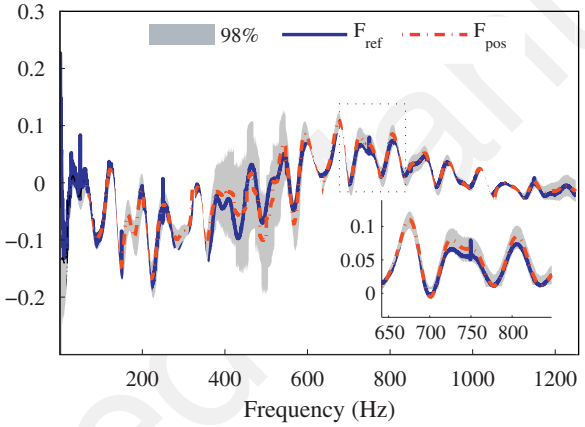

Fig. 20. Imaginary part (gray zone: 98 percent credible interval, $\mathbf{F}_{ref}$: reference force, $\mathbf{F}_{pos}$: posterior mean value of reconstructed force).

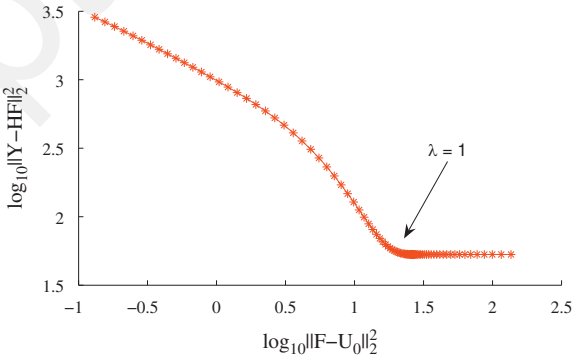

Fig. 21. L-curve.

credible interval can reflect this local lack of reliability contrary to a punctual estimation displayed alone. The Tikhonov regularization is also implemented with optimal value of λ found equal to 1 from the L-curve [6] as shown in Fig. 21. For comparison, the ratio $\sigma_N^2/\sigma_{F_0}^2(\omega)$ in the Bayesian approach plays the same regularization role, yet as a function of frequency as demonstrated in Fig. 22. The reconstructed forces in the time domain are compared in Fig. 23 for both methods. It is seen that the proposed method has a better accuracy than the standard Tikhonov method, especially in

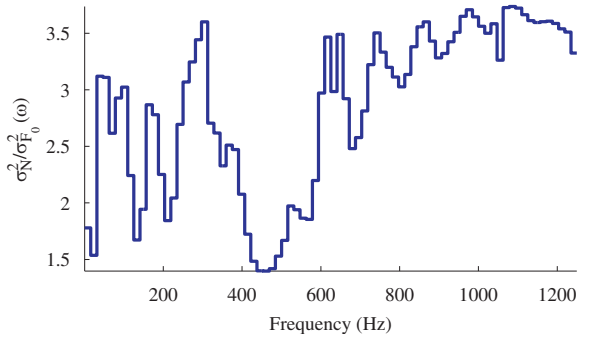

Fig. 22. Regularization parameter ($\sigma_N^2/\sigma_{F_0}^2(\omega)$).

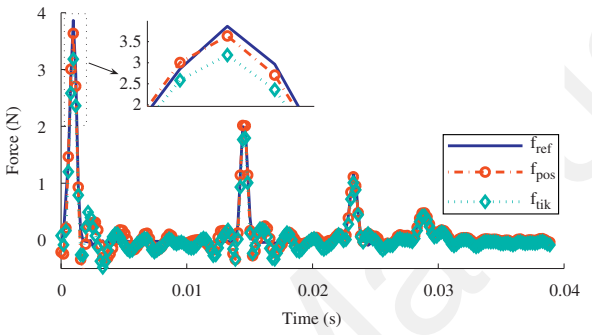

Fig. 23. Reconstructed force in the time domain ($\mathbf{f}_{ref}$ from the acquired measurement, $\mathbf{f}_{pos}$ by Bayesian approach and $\mathbf{f}_{tik}$ by Tikhonov regularization).

estimating the maxima of the force peaks. In addition, it should be remembered that the Bayesian approach returns the full posterior p.d.f. of the force which is a much richer amount of information than the punctual estimate of Eq. (11) alone.

6. Concluding remarks

A Bayesian force reconstruction methodology based on the inversion of an uncertain model has been proposed and validated on numerical and experimental examples. The main advantages of this approach lay in (1) accounting for all sources of uncertainty (measurement noise and modeling errors) in the same probabilistic framework, (2) incorporating a natural mechanism of regularization with automatic tuning as a function of frequency, (3) returning the full posterior probability distribution of the reconstructed force from which any statistics can be ultimately computed. One of the key points that make this approach feasible is its implementation by means of MCMC methods. As a perspective view to future work, the Bayesian approach seems well-suited to attack the more difficult problem of reconstructing *distributed* forces from uncertain structural models.

Appendix A. Joint, conditional and marginal p.d.f.'s and the circular complex normal distribution

A.1. Recall on joint, conditional and marginal probability distributions

The recall is illustrated in the case of three random variables (x_1,x_2,x_3). The joint p.d.f. is by definition written as $p(x_1,x_2,x_3)$.

- The conditional p.d.f. describes the probability of a group of parameters by fixing the rest at their known values, for instance, $p(x_1|x_2,x_3)$, which can be easily derived from $p(x_1,x_2,x_3)$ by considering x_2 and x_3 constant.
- The marginal p.d.f. of a variable is obtained from the joint p.d.f. by marginalizing out all the other parameters, for instance, $p(x_1) = \int p(x_1,x_2,x_3)\,\mathrm{d}x_2\,\mathrm{d}x_3$.
- A possible factorization by applying the total probability rule is $p(x_1,x_2,x_3) = p(x_1|x_2,x_3)p(x_2,x_3)$, which demonstrates the relation between the joint, conditional and marginal p.d.f.'s.
- x_1 and x_2 are mutually independent if and only if $p(x_1,x_2) = p(x_1)p(x_2)$.

A.2. Circular complex normal distribution

A complex-value variable $x = a + \jmath b$, with independent real-valued real and imaginary parts, $a \sim \mathcal{N}(a_0, \sigma_x^2/2)$ and $b \sim \mathcal{N}(b_0, \sigma_x^2/2)$, follows a so-called circular complex normal distribution:

$$p(x|x_0, \sigma_x^2) = \frac{1}{\pi\sigma_x^2} \exp(-(x-x_0)^*(x-x_0)/\sigma_x^2), \tag{A.1}$$

with $x_0 = a_0 + \jmath b_0$.

Appendix B. Detailed description of the conditional p.d.f.'s in Algorithm 1 of Section 3.3

B.1. Conditional p.d.f. of the force

$$p(\mathbf{F}|\sigma_N^{-2}, \mathbf{F}_0, \lceil C_{F_0}^{-1} \rfloor, \mathcal{D}) = p(\mathbf{F}, \sigma_N^{-2}, \mathbf{F}_0, \lceil C_{F_0}^{-1} \rfloor | \mathcal{D}) / p(\sigma_N^{-2}, \mathbf{F}_0, \lceil C_{F_0}^{-1} \rfloor | \mathcal{I}) = p([Y]|\mathbf{F}, \sigma_N^{-2}) p(\mathbf{F}|\mathbf{F}_0, \lceil C_{F_0}^{-1} \rfloor). \tag{B.1}$$

Hence $\ln(p(\mathbf{F}|\sigma_N^{-2}, \mathbf{F}_0, \lceil C_{F_0}^{-1} \rfloor, \mathcal{D}))$ is written as $-n_\omega n_s \ln \sigma_N^2 - \sum_{i=1}^{n_\omega} \ln \sigma_{F_0}^2(\omega_i) - \sum_{k=1}^{n_s} (\mathbf{Y}_k - \lceil H_k \rfloor \mathbf{F})^* (\mathbf{Y}_k - \lceil H_k \rfloor \mathbf{F}) / \sigma_N^2 - (\mathbf{F}-\mathbf{F}_0)^* \lceil C_{F_0}^{-1} \rfloor (\mathbf{F}-\mathbf{F}_0)$. Let the derivative $\partial \ln(p(\mathbf{F}|\sigma_N^{-2}, \mathbf{F}_0, \lceil C_{F_0}^{-1} \rfloor, \mathcal{D}))/\partial \mathbf{F}$ equal to zero; it returns that the optimal identified force $\hat{\mathbf{F}} = \lceil \hat{C}_F \rfloor (\sum_{k=1}^{n_s} \lceil H_k \rfloor^* \mathbf{Y}_k / \sigma_N^2 + \lceil C_{F_0}^{-1} \rfloor \mathbf{F}_0)$. Then $\partial^2 \ln(p(\mathbf{F}|\sigma_N^{-2}, \mathbf{F}_0, \lceil C_{F_0}^{-1} \rfloor, \mathcal{D}))/\partial \mathbf{F} \partial \mathbf{F}^*$ returns the posterior matrix covariance $\lceil \hat{C}_F \rfloor = (\sum_{k=1}^{n_s} \lceil H_k \rfloor^* \lceil H_k \rfloor / \sigma_N^2 + \lceil C_{F_0}^{-1} \rfloor)^{-1}$. As a result, $p(\mathbf{F}|\sigma_N^{-2}, \mathbf{F}_0, \lceil C_{F_0}^{-1} \rfloor, \mathcal{D}) = \mathcal{N}_c(\hat{\mathbf{F}}, \lceil \hat{C}_F \rfloor)$.

B.2. Conditional p.d.f. of the variance of measurement and model errors

$$\begin{aligned} p(\sigma_N^{-2}|\mathbf{F}, \mathcal{D}) = p([Y]|\mathbf{F}, \sigma_N^{-2}) p(\sigma_N^{-2}|\mathcal{I}) \propto (\sigma_N^{-2})^{(n_s n_\omega)} \exp\ & -\sigma_N^{-2} \sum_{k=1}^{n_s} (\mathbf{Y}_k - \lceil H_k \rfloor \mathbf{F})^* (\mathbf{Y}_k - \lceil H_k \rfloor \mathbf{F}) \Bigg) \\ \times (\sigma_N^{-2})^{(k_N - 1)} \exp(-\sigma_N^{-2} \beta_N) &\propto \Gamma(\hat{k}_N, \hat{\beta}_N) \end{aligned} \tag{B.2}$$

with $\hat{k}_N = (\sigma_N^{-2})^{(k_N + n_s n_\omega)}$ and $\hat{\beta}_N = (\beta_N + \sum_{k=1}^{n_s} (\mathbf{Y}_k - \lceil H_k \rfloor \mathbf{F})^* (\mathbf{Y}_k - \lceil H_k \rfloor \mathbf{F}))$.

B.3. Conditional p.d.f. of the prior mean value of the force

$$\begin{aligned} p(F_0(l)|\mathbf{F}_l, \sigma_{F_0}^{-2}(l)) \propto p(\mathbf{F}_l|F_0(l), \sigma_{F_0}^{-2}(l)) p(F_0(l)|U_0(l), \sigma_{U_0}^2) &\propto \exp(-(\mathbf{F}(l) - F_0(l)\mathbf{I}_l)^* (\mathbf{F}(l) - F_0(l)\mathbf{I}_l) \sigma_{F_0}^{-2}(l)) \\ \times \exp(-(F_0(l) - U_0)^* (F_0(l) - U_0) \sigma_{U_0}^{-2}) &\propto \mathcal{N}_c(\hat{U}_0, \hat{\sigma}_{U_0}^{-2}), \end{aligned} \tag{B.3}$$

where $\hat{\sigma}_{U_0}^2 = (|D_l| \sigma_{F_0(l)}^{-2} + \sigma_{U_0}^{-2})^{-1}$, $\hat{U}_0 = (\sigma_{F_0(l)}^{-2} \sum_{i \in D_l} F(\omega_i) + U_0 \sigma_{U_0}^{-2}) \hat{\sigma}_{U_0}^2$, $\mathbf{I}_l$ is the column vector of length $|D_l|$.

B.4. Conditional p.d.f. of the prior variance of the force

$$\begin{aligned} p(\sigma_{F_0}^{-2}(l)|\mathbf{F}(l), F_0(l)) \propto p(\mathbf{F}(l)|F_0(l), \sigma_{F_0}^{-2}(l)) p(\sigma_{F_0}^{-2}(l)|\mathcal{I}) &\propto (\sigma_{F_0}^{-2}(l))^{|D_l|} \exp(-(\mathbf{F}(l) - F_0(l)\mathbf{I}_l)^* (\mathbf{F}(l) - F_0(l)\mathbf{I}_l) \sigma_{F_0}^{-2}(l)) \\ \times (\sigma_{F_0}^{-2}(l))^{(k_F - 1)} \exp(-\beta_F \sigma_{F_0}^{-2}(l)) &\propto \Gamma(\hat{k}_F, \hat{\beta}_F) \end{aligned} \tag{B.4}$$

with $\hat{k}_F = k_F + |D_l|$ and $\hat{\beta}_F = \beta_F + (\mathbf{F}(l) - F_0(l)\mathbf{I}_l)^* (\mathbf{F}(l) - F_0(l)\mathbf{I}_l)$.

Appendix C. Description of Algorithm 2 of Section 4.2

C.1. Conditional p.d.f. of the coefficients of the force

$$\begin{aligned} p(\mathbf{X}|\mathcal{D}, \boldsymbol{\alpha}, \sigma_\eta^{-2}, \sigma_N^2) = \left\{ \int p([Y]|\mathbf{F}, \boldsymbol{\alpha}, \sigma_N^{-2}) p(\mathbf{F}|\mathbf{X}, \sigma_\eta^{-2})\, \mathrm{d}\mathbf{F} \right\} p(\mathbf{X}|\mathcal{I}) \propto & \int \exp\ -\sum_{k=1}^{n_s} (\mathbf{Y}_k - \lceil H_k(\boldsymbol{\alpha}) \rfloor \mathbf{F})^* (\mathbf{Y}_k - \lceil H_k(\boldsymbol{\alpha}) \rfloor \mathbf{F}) \sigma_N^{-2} \Bigg) \\ \times \exp(-(\mathbf{F} - [B]\mathbf{X})^* (\mathbf{F} - [B]\mathbf{X}) \sigma_\eta^{-2})\, \mathrm{d}\mathbf{F} &\propto \mathcal{N}_c(\hat{\mathbf{X}}, [\hat{C}_X]) \end{aligned} \tag{C.1}$$

with $[\hat{C}_X] = ([B]^* \lceil H_s(\boldsymbol{\alpha}) \rfloor^* (\lceil H_s(\boldsymbol{\alpha}) \rfloor^* \lceil H_s(\boldsymbol{\alpha}) \rfloor \sigma_\eta^2 + \sigma_N^2)^{-1} \lceil H_s(\boldsymbol{\alpha}) \rfloor [B])^{-1}$, $\lceil H_s(\boldsymbol{\alpha}) \rfloor = \sqrt{\sum_{k=1}^{n_s} \lceil H_k(\boldsymbol{\alpha}) \rfloor^* \lceil H_k(\boldsymbol{\alpha}) \rfloor}$, and $\hat{\mathbf{X}} = [\hat{C}_X][B]^* (\lceil H_s(\boldsymbol{\alpha}) \rfloor^* \lceil H_s(\boldsymbol{\alpha}) \rfloor \sigma_\eta^2 + \sigma_N^2)^{-1} \sum_{k=1}^{n_s} \lceil H_k(\boldsymbol{\alpha}) \rfloor^* \mathbf{Y}_k$.

C.2. Sample the modal parameters by Metropolis–Hastings algorithm

At i-th iteration during the MCMC sampling,

- generate a candidate by drawing $\boldsymbol{\alpha}' \sim q(\boldsymbol{\alpha}|\boldsymbol{\alpha}^{(i)})$
- calculate the acceptance probability

$$\gamma(\boldsymbol{\alpha}', \boldsymbol{\alpha}^{(i)}) = \min\left[\frac{p(\boldsymbol{\alpha}'|\mathbf{F}, \sigma_N^{-2}, \mathcal{D}) q(\boldsymbol{\alpha}^{(i)}|\boldsymbol{\alpha}')}{p(\boldsymbol{\alpha}^{(i)}|\mathbf{F}, \sigma_N^{-2}, \mathcal{D}) q(\boldsymbol{\alpha}'|\boldsymbol{\alpha}^{(i)})}, 1\right] \tag{C.2}$$

  with $p(\boldsymbol{\alpha}|\mathbf{F}, \sigma_N^{-2}, \mathcal{D}) \propto p([Y]|\boldsymbol{\alpha}, \mathbf{F}, \sigma_N^{-2}) p(\boldsymbol{\alpha}|\mathcal{I})$ and $q(\boldsymbol{\alpha})$ a proposal p.d.f., chosen by user.
- Accept or reject by drawing $t \sim \mathcal{U}(0,1)$, set

$$\boldsymbol{\alpha}^{(i+1)} = \begin{cases} \boldsymbol{\alpha}' & \text{if } t \leq \gamma(\boldsymbol{\alpha}', \boldsymbol{\alpha}^{(i)}), \\ \boldsymbol{\alpha}^{(i)} & \text{otherwise.} \end{cases} \tag{C.3}$$

References

[1] J. Antoni, J. Daniere, F. Guillet, Effective vibration analysis of ic engines using cyclostationarity. Part I—a methodology for condition monitoring, *Journal of Sound and Vibration* 257 (2002) 815–837.
[2] J. Mottershead, B. Datta, Special issue on inverse problems in mssp, *Mechanical Systems and Signal Processing* 23 (2009) 1731–1733.
[3] E. Jacquelin, A. Bennani, P. Hamelin, Force reconstruction: analysis and regularization of a deconvolution problem, *Journal of Sound and Vibration* 265 (2003) 81–107.
[4] Q. Leclère, C. Pezerat, B. Laulagnet, L. Polac, Indirect measurement of main bearing loads in an operating diesel engine, *Journal of Sound and Vibration* 286 (2005) 341–361.
[5] Y. Liu, W.S. Shepard Jr., Dynamic force identification based on enhanced least squares and total least-squares schemes in the frequency domain, *Journal of Sound and Vibration* 282 (2005) 37–60.
[6] H. Choi, A. Thite, D. Thompson, Comparison of methods for parameter selection in Tikhonov regularization with application to inverse force determination, *Journal of Sound and Vibration* 304 (2007) 894–917.
[7] C. Ma, J. Chang, D. Lin, Input forces estimation of beam structures by an inverse method, *Journal of Sound and Vibration* 259 (2003) 387–407.
[8] F. Gunawan, H. Homma, Y. Kanto, Two-step b-splines regularization method for solving an ill-posed problem of impact-force reconstruction, *Journal of Sound and Vibration* 297 (2006) 200–214.
[9] S. Granger, L. Perotin, An inverse method for the identification of a distributed random excitation acting on a vibrating structure part 1: theory, *Mechanical Systems and Signal Processing* 13 (1999) 53–65.
[10] Y. Liu, W.S. Shepard Jr., An improved method for the reconstruction of a distributed force acting on a vibrating structure, *Journal of Sound and Vibration* 291 (2006) 369–387.
[11] X. Jiang, H. Hu, Reconstruction of distributed dynamic loads on a thin plate via mode-selection and consistent spatial expression, *Journal of Sound and Vibration* 323 (2009) 626–644.
[12] J. Bendat, A. Piersol, *Engineering Applications of Correlation and Spectral*, Wiley, 1993.
[13] D. Ewins, *Modal Testing: Theory, Practice and Application*, Wiley, 2001.
[14] M. Friswell, J. Mottershead, *Finite Element Model Updating in Structural Dynamics*, Kluwer Academic Publishers, Dordrecht, 1995.
[15] Y. Kim, K. Kim, Indirect input identification by modal filter technique, *Mechanical Systems and Signal Processing* 13 (1999) 893–910.
[16] P. Lee, *Bayesian Statistics: An Introduction*, Arnold Publication, 1997.
[17] A. Tarantola, *Inverse Problem Theory and Methods for Model Parameter Estimation*, SIAM (Society of Industrial and Applied Mathematics), 2005.
[18] J. Rice, *Mathematical Statistics and Data Analysis*, Duxbury Press, 1995.
[19] R. Pintelon, J. Schoukens, *System Identification: A Frequency Domain Approach*, Wiley, IEEE Press, 2001.
[20] A. Tychonoff, V. Arsenin, *Solution of Ill-Posed Problems*, Winston & Sons, Washington, 1977.
[21] W. Hastings, Monte Carlo sampling methods using Markov chains and their applications, *Biometrika* 57 (1970) 97–109.
[22] S. Geman, D. Geman, Stochastic relaxation, Gibbs distributions and the Bayesian restoration of images, *IEEE Transactions on Pattern Analysis and Machine Intelligence* 6 (1984) 721–741.
[23] W. Gilks, S. Richardson, D. Spiegelhalter, *Markov Chain Monte Carlo in Practice*, Chapman and Hall, 1995.
[24] M. Chen, Q. Shao, J. Ibrahim, *Monte Carlo Methods in Bayesian Computation*, Springer, 2000.
[25] K.V. Yuen, *Bayesian Methods for Structural Dynamics and Civil Engineering*, Wiley, 2010.
[26] C. Robert, G. Casella, *Monte Carlo Statistical Methods*, 2nd ed., Springer, 2004.
[27] E. Zhang, Inverse Problem in Structural Dynamics Within Bayesian Framework: Model Updating and Force Reconstruction, PhD Thesis, Université de Techonologie de Compiègne, 2010 (in French).